



Research Paper

Influence of chemical exfoliation process on the activity of $\text{NiCl}_2\text{-FeCl}_3\text{-PdCl}_2$ -graphite intercalation compound towards methanol electrooxidation

T. Rozmanowski*, P. Krawczyk

Poznan University of Technology, Institute of Chemistry and Technical Electrochemistry, ul. Berdychowo 4, 60-965 Poznań, Poland

ARTICLE INFO

Keywords:

Graphite intercalation compounds

Exfoliation

Palladium catalyst

Methanol electrooxidation

ABSTRACT

In the present work the influence of chemical exfoliation process of quaternary graphite intercalation compound ($\text{NiCl}_2\text{-FeCl}_3\text{-PdCl}_2\text{-GIC}$) on its catalytic activity in the methanol electrooxidation reaction was examined. $\text{NiCl}_2\text{-FeCl}_3\text{-PdCl}_2\text{-GIC}$ was synthesized by a molten salts method using purified flaky graphite and anhydrous metal chlorides as reactants. The process of intercalation was carried out at 450 °C for 72 h. To obtain exfoliated graphite intercalation compound ($\text{NiCl}_2\text{-FeCl}_3\text{-PdCl}_2\text{-EGIC}$), a part of gathered product underwent chemical exfoliation in hydrogen peroxide solution. Crystalline structure of the obtained GIC and product of its exfoliation was characterized by XRD while their morphology by SEM and TEM techniques. Development of the surface area was calculated by BET method. Electrochemical activity of both materials were examined in the model process of methanol electrooxidation by cyclic (CV) and linear sweep (LSV) voltammetry as well as potentiostatic method.

The XRD and SEM analysis have showed that the chemical exfoliation process contributes to the changes in structure and morphology of the examined material.

From the electrochemical results it is revealed that prepared $\text{NiCl}_2\text{-FeCl}_3\text{-PdCl}_2\text{-GIC}$ exhibits activity towards electrochemical process of methanol oxidation. Furthermore is proved that electroactivity of the examined $\text{NiCl}_2\text{-FeCl}_3\text{-PdCl}_2\text{-GIC}$ significantly increases due its chemical exfoliation.

1. Introduction

Electrochemical oxidation of small organic molecules of low molecular weight is widely considered as a fundamental process in new source of energy like alcohol fuel cells [1–3]. The greatest attention is focused on Direct Methanol Fuel Cells (DMFCs), in which methanol is used as a fuel. Methanol is common fuel regarded in chemical industry with high energy density, theoretically even up to 6.0 Wh g⁻¹ [4]. Due to its easily storage methods in comparison to hydrogen fuel, methanol is also considered as a potential effective fuel for portable devices. The process of anodic oxidation of methanol in DMFCs generates electric energy which is accompanied by the formation of products like water and carbon dioxide. The crucial role plays the material employed as the anodic catalysts. It is known that highest activity in the process of methanol electrooxidation exhibits Pt-Ru catalyst with a Pt:Ru atomic ratio of 1:1 [5,6]. However due to high cost of platinum as well as ruthenium catalysts a new type of anodic materials-catalyst are desirable.

One of the catalyst being in the wide spectrum of interest as electrode material for methanol electrooxidation is palladium [7–10].

Contrary to platinum, Pd is more abundant in nature hence its cost is significantly lower than Pt. Furthermore, it has been proved by Antolini et al. [11] that palladium is a better catalyst for alcohol electrooxidation in alkaline media than Pt. Alkaline electrolyte enables an application of second or third non-noble metals being stable in alkaline media thus enhancing the total activity of alloyed catalyst towards alcohol electrooxidation [12].

Another important factor influencing the efficiency of methanol oxidation is specific surface area of the anodic catalyst. In order to enhance anode electroactivity, the metallic catalyst is deposited onto the carbon support characterized by the well developed specific surface area [13–15]. Those solution not only imply the enhancement of catalyst activity but also results in significantly reduction of its cost. One of the group of materials which fulfills above mentioned requirements are graphite intercalation compounds (GIC). GIC can be obtained by the insertion of ions and/or molecules, e.g., alkali metals, metal oxides or transition metal chlorides between the graphene layers where are chemically bounded with a carbon matrix [16–19]. It has been reported by many workers that it is possible to obtain GIC containing more than one type of intercalate occupied the interlayer space in graphen sheets

* Corresponding author.

E-mail address: tomasz.rozmanowski@put.poznan.pl (T. Rozmanowski).

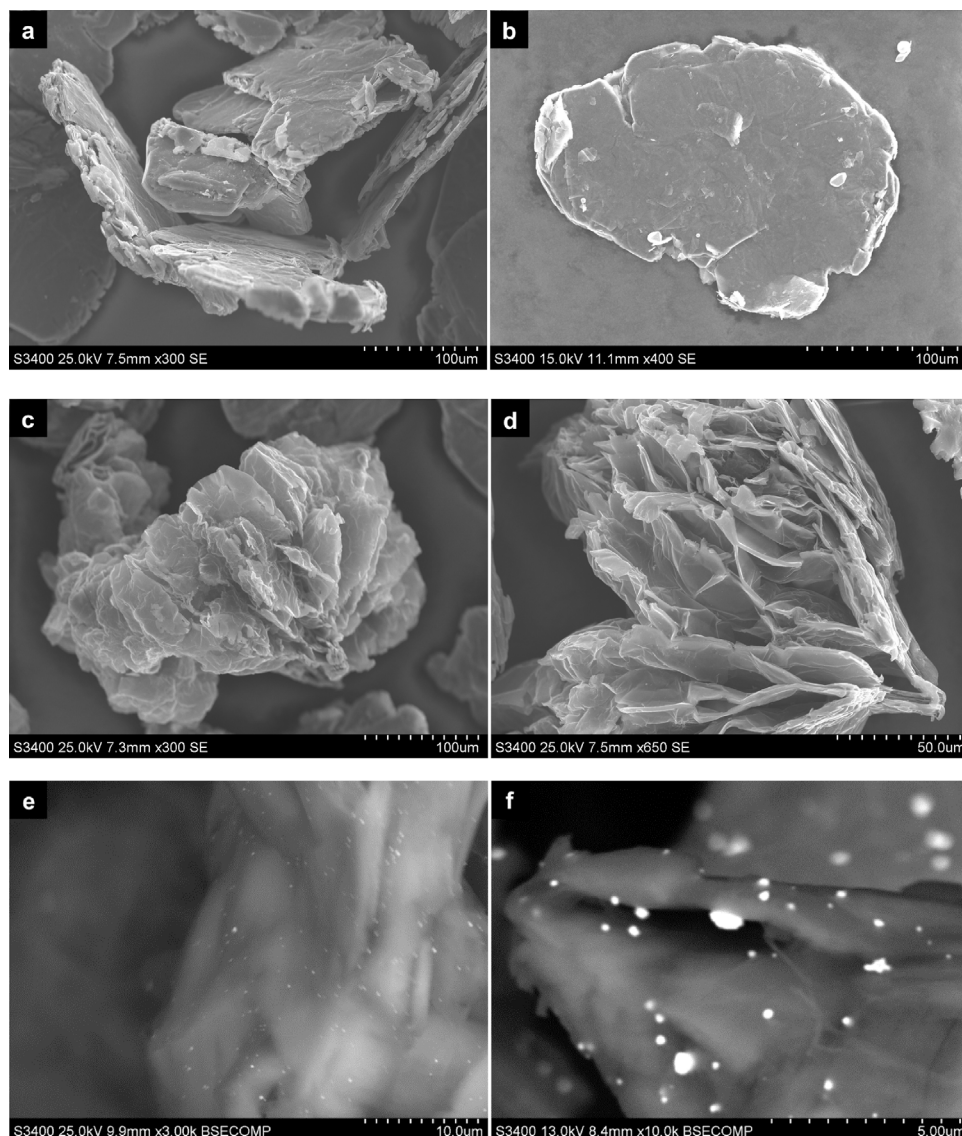


Fig. 1. SEM images of the original $\text{NiCl}_2\text{-FeCl}_3\text{-PdCl}_2\text{-GIC}$ (a and b) and $\text{NiCl}_2\text{-FeCl}_3\text{-PdCl}_2\text{-EGIC}$ (c–f).

thus widening the range of its potential application [20–22]. Most of graphite intercalation compounds easily undergo exfoliation [23]. This process can be realized by thermal [24], chemical [25] or electrochemical [26] methods. The exfoliation process takes place due to entire or partial decomposition of intercalate molecules followed by the release of gathered gaseous products. Rapid eruption of gases from graphite lattice causes multiple splitting and wrinkling of graphite flakes leading to its expansion along the c-axis and in consequence a tremendous modification of graphite structure [23]. Graphite compounds, in which some part of intercalate is preserved with the graphite lattice after the exfoliation are recognized as exfoliated graphite intercalation compound (EGIC) [23,27].

The present paper explains the influence of chemical exfoliation of $\text{NiCl}_2\text{-FeCl}_3\text{-PdCl}_2\text{-graphite}$ intercalation compound on its structural, morphological and electrochemical properties. Electrochemical behavior of the obtained material was investigated basing on the processes of methanol electrooxidation performed in alkaline media.

2. Materials and methods

The synthesis of $\text{NiCl}_2\text{-FeCl}_3\text{-PdCl}_2\text{-GIC}$ was carried out by molten salt method, in which purified flaky graphite (99.98 wt.% C, flakes 100 μm in diameter) and anhydrous chlorides of Ni, Fe and Pd were

used as a substrates. The molar ratio of metal salts to graphite was adjusted to 1:3, whereas the molar ratio of $\text{NiCl}_2\text{:FeCl}_3\text{:PdCl}_2$ was equal to 5:3:2. Process of intercalation was carried out in glass reactor at 450 $^\circ\text{C}$ for 72 h in argon atmosphere. To remove unreacted salts the synthesized GIC was filtered and washed with diluted HCl solution, than the obtained product was rinsed with water and dried in air at ambient temperature. Part of as prepared $\text{NiCl}_2\text{-FeCl}_3\text{-PdCl}_2\text{-GIC}$ was subjected to chemical exfoliation by immersion in 30% solution of hydrogen peroxide for 2 h at 25 $^\circ\text{C}$. The acquired product of this process is defined as exfoliated graphite intercalation compound and named throughout the paper as $\text{NiCl}_2\text{-FeCl}_3\text{-PdCl}_2\text{-EGIC}$, abbreviated in Figures to EGIC.

The crystalline structure and morphology of both original and chemically exfoliated GIC was characterized by X-ray diffraction (XRD) measurements (Philips PW-1710 diffractometer) and scanning electron microscopy (SEM) (Hitachi S-3400N) equipped with EDS detector as well as transmission electron microscopy (TEM) (Jeol 1200 EX2), respectively. Development of the surface area was estimated by BET method (ASAP 2010 V2.00C).

Electrochemical measurements were performed at ambient temperature by cyclic voltammetry (CV), linear sweep voltammetry (LSV) and potentiostatic method using a potentiostat-galvanostat PGSTAT30 AutoLab (EcoChemie B.V.). For electrochemical experiments, the

electrode material was placed into a pocket made of porous polymer material, in which graphite rod (5 mm in diameter) playing a role of current collector was beforehand inserted. CV measurements were carried out in a three-electrode cell filled with 6 M KOH solution. During the process of methanol electrooxidation, 1.0 M methanol dissolved in 6 M KOH was used as an electrolyte. A Hg/HgO/6 M KOH (0.098 V vs. NHE) serve as the reference electrode, whereas a platinum gauze was a counter electrode. CV measurements were performed in the potential range $-1.1 \leftrightarrow 0.3$ V with scan rate 10 mV s^{-1} , starting from the rest potential of electrode towards the negative potentials. In some experiments, when the electrode reached the potential of -1.1 V, the scanning was stopped for 15 min to perform a potentiostatic saturation of electrode with hydrogen. Afterwards, the potential scanning was continued in the positive direction. To verify the electroactivity of examined electrodes the potentiostatic measurements were conducted at constant potential value of 0.6 V.

3. Results and discussion

3.1. Characterization of the investigated materials

3.1.1. SEM analysis

The morphology of the original $\text{NiCl}_2\text{-FeCl}_3\text{-PdCl}_2\text{-GIC}$ and $\text{NiCl}_2\text{-FeCl}_3\text{-PdCl}_2\text{-EGIC}$ can be observed on SEM images placed in Fig. 1a, b and c, d, respectively. From Fig. 1a it can be seen that host $\text{NiCl}_2\text{-FeCl}_3\text{-PdCl}_2\text{-GIC}$ is composed of flat flakes without any signs of exfoliation. The cracked character of graphite flakes is associated with the invasion of intercalate molecules into the interlayer space between the graphene layers. Chemical interactions between $\text{NiCl}_2\text{-FeCl}_3\text{-PdCl}_2\text{-GIC}$ and 30% hydrogen peroxide solution result in partial splitting and wrinkling of graphite flakes, leading to the formation of product of accordion-like structure (Fig. 1c and d). The above mentioned observations justify the conclusion that due to oxidation of metal chlorides by hydrogen peroxide accompanied by the oxygen and chloride evolution, the process of exfoliation takes place. Irregular shape of exfoliated graphite flakes especially visible in Fig. 1d can be assigned to different speed of chemical exfoliation being correlated with uneven distribution of intercalate particles within graphitic matrix. Figs. 1e and f show SEM images for $\text{NiCl}_2\text{-FeCl}_3\text{-PdCl}_2\text{-EGIC}$ recorded under higher magnification with use of back scattered electrons (BSE) detector. This allows to distinguish intercalate particles from graphitic matrix. As can be seen, bright spots representing agglomerates of intercalate molecules are evenly distributed on the graphite matrix. From Fig. 1f it can be concluded that above mentioned aggregates have diameters varying from 100 nm to 1 μm .

Detailed analysis of both materials performed by transmission electron microscopy (Fig. 2) proves that particles of intercalate, which are visible as a dark spots on TEM images exhibit diameter ranged between 1 and 100 nm.

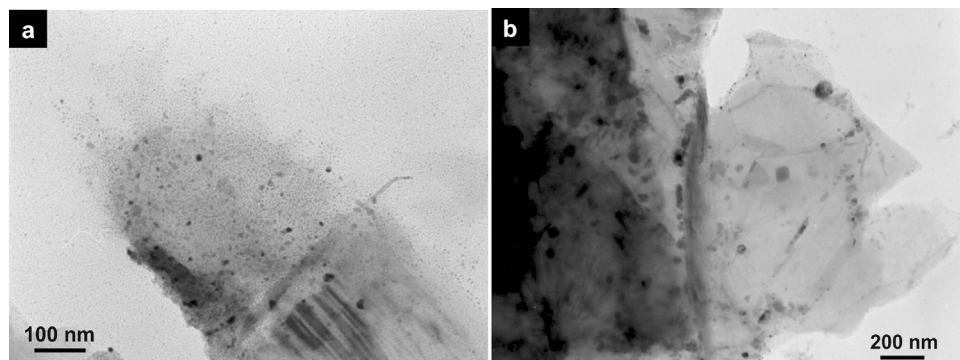


Fig. 2. TEM images of the original $\text{NiCl}_2\text{-FeCl}_3\text{-PdCl}_2\text{-GIC}$ (a) and $\text{NiCl}_2\text{-FeCl}_3\text{-PdCl}_2\text{-EGIC}$ (b).

Table 1

Chemical composition of $\text{NiCl}_2\text{-FeCl}_3\text{-PdCl}_2\text{-GIC}$ and $\text{NiCl}_2\text{-FeCl}_3\text{-PdCl}_2\text{-EGIC}$ based on EDS analysis [at.%].

	C	O	Cl	Ni	Pd	Fe
GIC	63.1	1.8	23.7	9.1	0.8	1.5
EGIC	56.7	7.5	21.8	10.2	2.6	1.2

3.1.2. EDS analysis

Chemical composition of the surface of obtained compounds calculated from EDS analysis is given in Table 1.

The presented data confirmed that intercalate within the original $\text{NiCl}_2\text{-FeCl}_3\text{-PdCl}_2\text{-GIC}$ appears in form of metal chlorides. This statement is revealed by the fact that the atomic percentage of chlorine 23.7 ± 0.8 at.% well matches the total amount of chlorine calculated from the chemical formulas of Ni, Pd and Fe chlorides (23.71 at.%). It should be noted that the total molar ratio of metal salts to graphite as well as the reciprocal molar ratio of metal chlorides differs from the original mixture. Decrease in molar ratio of metal salts to graphite is caused by the fact, that only part of chlorides used for preparation of reaction mixture undergoes intercalation. This effect is typical for such type of intercalation processes, in which a great excess of reactants related to graphite is used to reach the high efficiency of intercalation process [23]. EDS analysis has also revealed the presence of small amount of oxygen within the product of intercalation, which is likely affected by the reaction of graphitic matrix with air upon evacuation of the compound from the reactor.

Chemical exfoliation of $\text{NiCl}_2\text{-FeCl}_3\text{-PdCl}_2\text{-GIC}$ results in a significant increase in atomic percentage of oxygen with simultaneous decrease in concentration of chlorine. Such a behavior may be assigned to the oxidation of graphitic matrix and intercalate molecules by active oxygen violently liberated during the catalytic decomposition of hydrogen peroxide. In consequence, the formation of oxygen containing functional groups on surface of exfoliated graphite flakes and partial transformation of intercalate into its oxide form probably occur. It should be also emphasized that the process of GIC exfoliation led to increase in atomic ratio of Pd to Ni and Fe. This effect can be ascribed to the splitting of graphene layers thus making an access to active species of intercalates easier.

3.1.3. XRD and BET analysis

Changes within the structure of ternary $\text{NiCl}_2\text{-FeCl}_3\text{-PdCl}_2\text{-GIC}$ affected by chemical exfoliation are confirmed by the XRD analysis (see Fig. 3). As it is shown in Fig. 3 (red line) the starting graphite intercalation compound with nickel, iron and palladium chlorides can be recognized as a mixture of stage-3, 4 compound (intercalation stage defined as number of graphene layers contained between two adjacent intercalate layers). This XRD pattern undoubtedly proves that pristine graphite was fully converted to GIC which is demonstrated by the lack of graphite diffraction peaks. Chemical exfoliation of $\text{NiCl}_2\text{-FeCl}_3\text{-PdCl}_2\text{-GIC}$ results in significant decrease in intensity of all

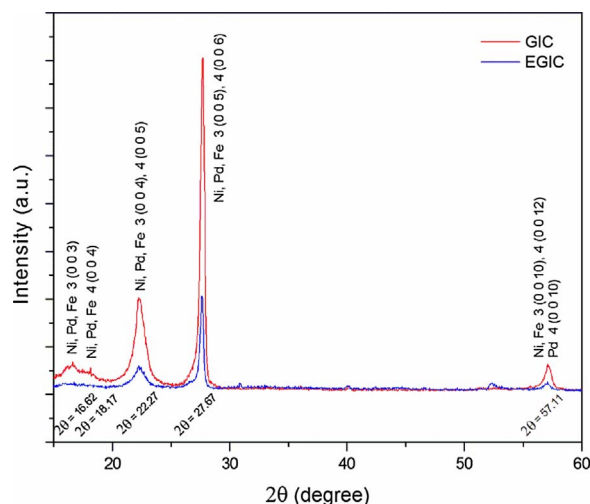


Fig. 3. Influence of exfoliation process on the structure of $\text{NiCl}_2\text{-FeCl}_3\text{-PdCl}_2\text{-GIC}$. The numbers placed before the brackets denote stage number of investigated GIC. (For interpretation of the references to colour in the text, the reader is referred to the web version of this article.)

intercalation peaks (Fig. 3, black line). This effect is most likely associated with the partial decomposition of intercalate molecules accompanied by the changes in graphitic structure caused by expansion of graphite flakes along the crystallographic axis c [23,28]. It should be noted that in spite of the diminution of peak intensity the XRD pattern for exfoliated GIC consist of diffraction peaks, which indicate that part of intercalate still remains in the same domains (stage-3,4) as for original $\text{NiCl}_2\text{-FeCl}_3\text{-PdCl}_2\text{-GIC}$. Therefore, the product of exfoliation can be recognized as exfoliated graphite intercalation compound (EGIC), not exfoliated graphite.

The development of the surface area of $\text{NiCl}_2\text{-FeCl}_3\text{-PdCl}_2\text{-GIC}$ caused by its chemical exfoliation was determined by BET method. The obtained results shows significant increase of specific surface area for original GIC from 0.412 to $8.023 \text{ m}^2 \text{ g}^{-1}$ for sample after chemical exfoliation. The obtained value of $8.023 \text{ m}^2 \text{ g}^{-1}$ is much lower than that noted for carbon porous material. It should be emphasized that despite some changes in chemical composition of $\text{NiCl}_2\text{-FeCl}_3\text{-PdCl}_2\text{-EGIC}$ the intercalate still persist within the graphite matrix, hence the developing of surface area is hindered. It is known that if the intercalate is abruptly released due to exfoliation, the modification of graphite structure occurs with accompaniment of development of specific surface area. In our case, during the chemical exfoliation of $\text{NiCl}_2\text{-FeCl}_3\text{-PdCl}_2\text{-GIC}$ only small amount of chlorine is remove from its structure resulting increase in specific surface area from 0.412 to $8.023 \text{ m}^2 \text{ g}^{-1}$.

3.2. Electrochemical measurements

3.2.1. Electrooxidation of methanol on GIC

Fig. 4 displays cyclic voltammograms (CV) for original $\text{NiCl}_2\text{-FeCl}_3\text{-PdCl}_2\text{-GIC}$ recorded in 6 M KOH solution with and without addition of 1 M methanol. For the presentation were selected 20th cycles of methanol oxidation. In case of CV curve recorded in methanol free electrolyte (red line), after starting from the rest potential of electrode (ER) in the negative direction, a slight increase of a cathodic current density is observed. This effect is most likely related with the reduction of surface functional groups (oxygen or/and chlorine) originally present at the surface of multi-graphene sheets [29,30]. When the potential reached -0.7 V abrupt increase in cathodic current density corresponding to the hydrogen evolution reaction and metal chlorides reduction is seen [25].

According to the literature data, it cannot be excluded that over the potential of -0.7 V , the hydrogen sorption in palladium also takes

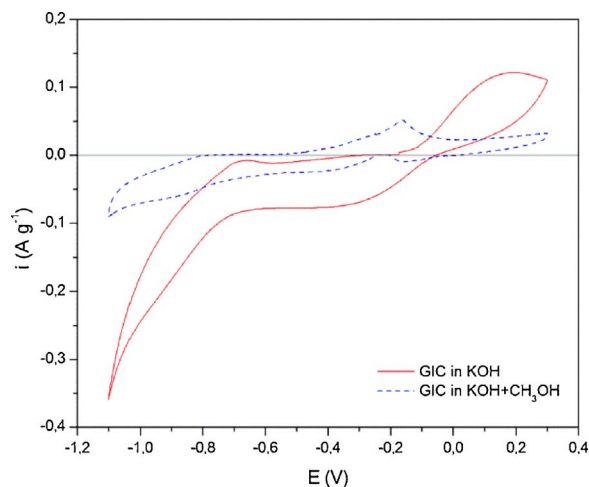


Fig. 4. Cyclic voltammograms for original $\text{NiCl}_2\text{-FeCl}_3\text{-PdCl}_2\text{-GIC}$ recorded in 6 M KOH solution with and without addition of methanol. Scan rate 10 mV s^{-1} . (For interpretation of the references to colour in the text, the reader is referred to the web version of this article.)

place [15,31,32]. After reversal the polarization at -1.1 V , barely visible anodic peak with maximum at -0.68 V is recorded. This peak can be ascribed to the hydrogen desorption and/or nickel oxidation [22,32]. On continuing anodic scanning another current peak spreading within the potential range of $-0.1 \text{ V} \leftrightarrow 0.3 \text{ V}$ is observed. The mentioned peak can be assigned to the oxidation of the surface of graphite matrix [30]. It should be noted that the intensity of this peak gradually diminishes on cycling (curves not presented in the manuscript) hence it is concluded that the process of surface oxidation is irreversible under the employed experimental conditions. The course of CV curve recorded for $\text{NiCl}_2\text{-FeCl}_3\text{-PdCl}_2\text{-GIC}$ electrode significantly changes after methanol addition to the base electrolyte. Cathodic as well as anodic signals correlated with the reduction and oxidation of graphite matrix almost completely disappear due to screening effect of methanol. Molecules of methanol are adsorbed at the surface of electrode thus covering its active parts. For the same reason, current density of hydrogen evolution/sorption reaction is over three times lower in comparison to this noted for the electrolyte free of methanol. During the anodic scanning a small anodic peak at -0.175 V associated with the methanol oxidation on Pd catalyst emerges [33,34]. A characteristic feature of voltammetric oxidation of methanol at Pd catalyst is a small anodic peak recorded during the cathodic polarization at -0.20 V . This peak is related to the reactivation of electrode surface [33].

3.2.2. Electrooxidation of methanol on EGIC

As it is shown in Fig. 5, the chemical exfoliation of $\text{NiCl}_2\text{-FeCl}_3\text{-PdCl}_2\text{-GIC}$ has a significant influence on its electrochemical behavior.

On regarding the measurement in KOH electrolyte free of methanol (red line) the most pronounced changes are observed during the anodic polarization. There is no signals correlated with reduction of surface functional groups. On the other hand, it is reasonable to emphasize that although the current density of hydrogen sorption/evolution reaction remains almost unchanged in comparison to that noted for non-exfoliated GIC (Fig. 4), the intensity of anodic peak corresponding to the hydrogen desorption is significantly higher. Moreover, the regarded peak becomes split into two maxima due to exfoliation of electrode material. Chemical treatment of $\text{NiCl}_2\text{-FeCl}_3\text{-PdCl}_2\text{-GIC}$ also reduced its susceptibility to electrochemical oxidation, depicted as a disappearance of anodic peak previously seen in Fig. 4. Experiments performed in electrolyte containing methanol showed, that activity of graphite intercalation compound in the reaction of electrochemical methanol oxidation significantly increase due to its exfoliation (Figs. 4 and 5, blue line). The process occurs within two overlapping peaks spreading

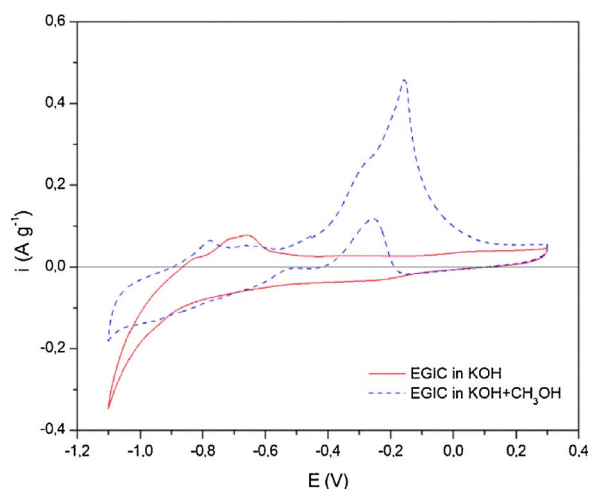


Fig. 5. Cyclic voltammograms for $\text{NiCl}_2\text{-FeCl}_3\text{-PdCl}_2\text{-EGIC}$ recorded in 6 M KOH solution with and without addition of methanol. Scan rate 10 mV s^{-1} . (For interpretation of the references to colour in the text, the reader is referred to the web version of this article.)

between the potentials of -0.58 V and 0.13 V . Such a behavior is probably associated with the multistep character of methanol electro-oxidation over the palladium catalyst. In case of $\text{NiCl}_2\text{-FeCl}_3\text{-PdCl}_2\text{-EGIC}$ current density of the main anodic peak (-0.18 V) is over 9-fold higher compared to that recorded for not exfoliated compound (Fig. 3) (increase from 0.05 to 0.46 A g^{-1}). Anodic charge related with the methanol oxidation increases from 0.63 C g^{-1} for original GIC to 9.42 C g^{-1} for chemically exfoliated compound. It gives almost 15-fold rise of the electrochemical activity in the regarded process. Moreover, anodic peak corresponding to the reactivation of electrode surface, recorded during the backward scanning becomes significantly greater. For huge increase in electrochemical activity of exfoliated compound towards the methanol oxidation the development of its active surface area is responsible (see section 3.1.3). This effect seems to be accompanied by the splitting of graphene layers facilitating on access of methanol molecules to active species of intercalates, especially Pd expelled from the graphite interspacing. The above statement remains in coincidence with the results of EDS analysis described in section 3.1.2.

In the next order, durability and stability of $\text{NiCl}_2\text{-FeCl}_3\text{-PdCl}_2\text{-GIC}$ and $\text{NiCl}_2\text{-FeCl}_3\text{-PdCl}_2\text{-EGIC}$ electrodes were examined by long-lasting CV measurements performed in $1 \text{ M CH}_3\text{OH}/6 \text{ M KOH}$. The dependence of current density of methanol oxidation peak on number of cycles performed is depicted in Fig. 6.

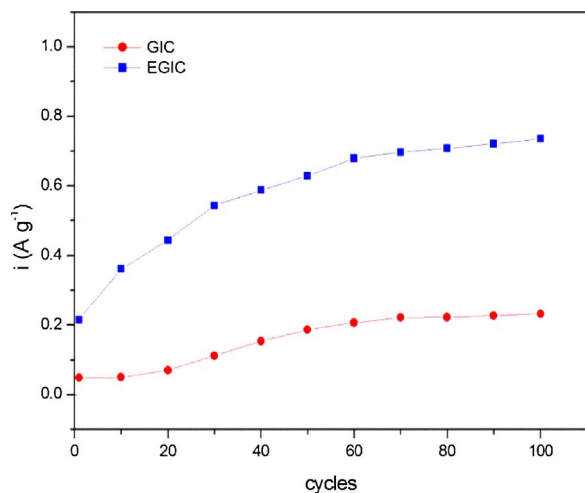


Fig. 6. Durability and stability of $\text{NiCl}_2\text{-FeCl}_3\text{-PdCl}_2\text{-GIC}$ and $\text{NiCl}_2\text{-FeCl}_3\text{-PdCl}_2\text{-EGIC}$ examined by long-term CV measurements in $1 \text{ M CH}_3\text{OH}/6 \text{ M KOH}$ solution.

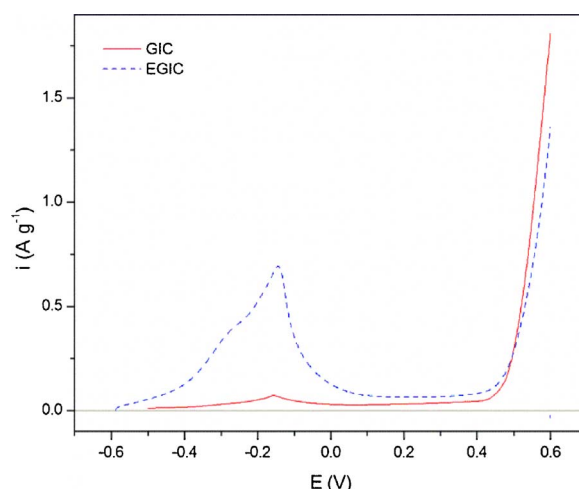


Fig. 7. Linear sweep voltammetry curves for $\text{NiCl}_2\text{-FeCl}_3\text{-PdCl}_2\text{-GIC}$ and $\text{NiCl}_2\text{-FeCl}_3\text{-PdCl}_2\text{-EGIC}$ recorded in $1 \text{ M CH}_3\text{OH}/6 \text{ M KOH}$ solution with scan rate 10 mV s^{-1} .

Current density of methanol oxidation peak increases upon cycling for both investigated materials. This effect is clearly visible during up to forty cycles. Such behavior can be likely associated with improvement in wettability of the examined electrodes along the cycling. On the other hand, it cannot be excluded that during the multiply repeated cycles, electrochemical exfoliation accompanied by the partial modification of graphite structure takes place. These structural changes in electrode facilitate on access of active centers to methanol molecules, thus rising their electroactivity. No signs of electrode deactivation upon cycling indicate good resistivity of the examined catalysts to poisoning effect caused by intermediate products of methanol oxidation. The entire explanation of the above described phenomena requires further examination including structural and morphological properties of electrode materials during and after long-term CV measurements.

3.2.3. Electrooxidation of methanol by LSV method

In order to understand the influence of exfoliation process on electroactivity of the $\text{NiCl}_2\text{-FeCl}_3\text{-PdCl}_2\text{-EGIC}$, the linear sweep voltammetry (LSV) and potentiostatic measurements were performed. As can be seen from Fig. 7 depicting LSV curves, the highest current density of methanol oxidation for both examined compounds is noted at potential of 0.6 V . This can be assigned to the catalytic effect of nickel catalyst (Ni^{3+}) [35]. Basing on LSV results, the potential of 0.6 V was selected for the potentiostatic measurements.

3.2.4. Electrooxidation of methanol by potentiostatic method

Potentiostatic curves for ternary $\text{NiCl}_2\text{-FeCl}_3\text{-PdCl}_2\text{-GIC}$ before and after chemical exfoliation recorded in 6 M KOH solution with and without addition of methanol are presented in Fig. 8. As it can be seen on all curves, after initial drop of current density correlated with a rapid polarization of examined electrode by under a constant potential of 0.6 V the current plateau is reached.

For both examined electrodes an addition of methanol to the basic electrolyte led to the increment in registered current density caused by alcohol oxidation. For non-exfoliated GIC, the current density grown from 0.28 A g^{-1} to 0.34 A g^{-1} . Much more pronounced increase is observed for graphite intercalation compound underwent chemical exfoliation. In this case, the average current density reached 1.25 A g^{-1} and is over 2 times higher compared to the measurement in which methanol was not oxidized (0.55 A g^{-1}). It is also almost 4 times higher in comparison to the current density achieved for original $\text{NiCl}_2\text{-FeCl}_3\text{-PdCl}_2\text{-GIC}$ in $1 \text{ M CH}_3\text{OH}/6 \text{ M KOH}$ solution. The frayed nature of potentiostatic curves recorded in methanol containing electrolyte can be ascribed to the gaseous CO_2 evolution being a final product of the alcohol oxidation. Anodic density charges calculated on the basis of

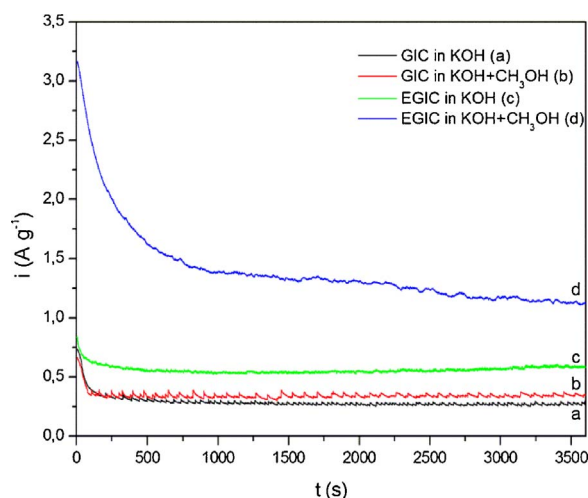


Fig. 8. Potentiostatic curves for $\text{NiCl}_2\text{-FeCl}_3\text{-PdCl}_2\text{-GIC}$ and $\text{NiCl}_2\text{-FeCl}_3\text{-PdCl}_2\text{-EGIC}$ recorded at 0.6 V in 6 M KOH with and without methanol addition.

Table 2

Density of anodic charges calculated from the potentiostatic measurements.

	Density of anodic charge Q_A [C g^{-1}]		
	KOH (Q_{A1})	KOH/ CH_3OH (Q_{A2})	$Q_{A2} - Q_{A1}$
GIC	1040	1243	203
EGIC	2023	5056	3033

potentiostatic curves are given in Table 2.

As can be seen from Table 2, calculated density of anodic charges for both materials examined in electrolyte with alcohol additive are significantly higher due to electrochemical oxidation. The anodic charges calculated for original GIC and exfoliated one correlated with methanol oxidation equals to 203 and 3033 C g^{-1} , respectively. It should be emphasized, that exfoliation caused 15-fold increase in anodic charge associated with methanol oxidation, while increase in total charges noted both for electrolyte with and without addition of methanol ($Q_{A2} - Q_{A1}$) is much less pronounced (Q_{A1} and Q_{A2} are only 4 and 2-fold higher, respectively). This observation leads to a conclusion, that chemical exfoliation of $\text{NiCl}_2\text{-FeCl}_3\text{-PdCl}_2\text{-GIC}$ not only modify its active surface area but also makes intercalate particles more accessible to methanol molecules.

Summarizing, performed potentiostatic measurements are consistent with CV results proving that the chemical exfoliation of $\text{NiCl}_2\text{-FeCl}_3\text{-PdCl}_2\text{-GIC}$ significantly impresses its catalytic activity towards methanol oxidation.

3.2.5. Electrooxidation of methanol and hydrogen sorption

In the last step of electrochemical investigation, the influence of saturation of examined electrodes with hydrogen on their electrochemical activity towards methanol oxidation was examined.

During the CV measurements, when electrode reached vertex potential of -1.1 V , the potential scanning was stopped for 15 min to saturate the electrode with hydrogen, afterwards the potential scanning was continued to the positive direction. The obtained CV curves for original and exfoliated graphite intercalation compound are given in Fig. 9 and 10, respectively. For both examined materials, potentiostatic treatment led to the formation of anodic peak with maximum at -0.58 V recorded during anodic polarization. This effect corresponds to desorption of hydrogen preceded by its accumulation in the electrodes during the potentiostatic sorption [36,37]. It is worth to note that the hydrogen sorption/desorption process caused significant increase in anodic charge of methanol oxidation peaks. Due to partial

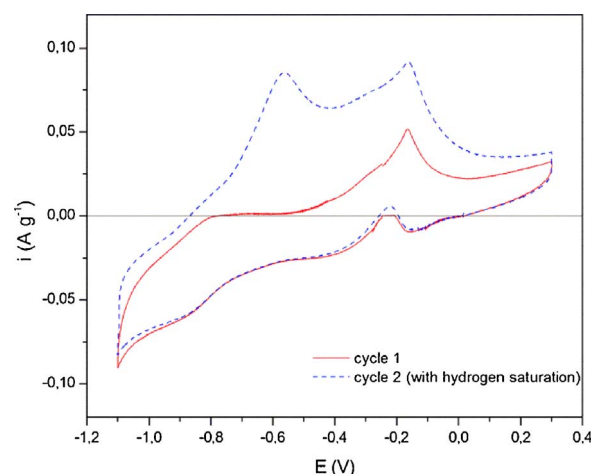


Fig. 9. Cyclic voltammograms recorded for original $\text{NiCl}_2\text{-FeCl}_3\text{-PdCl}_2\text{-GIC}$ in 6 M KOH solution with and without addition of methanol accompanied by the 15 min hydrogen saturation of electrode at -1.1 V . Scan rate 10 mV s^{-1} .

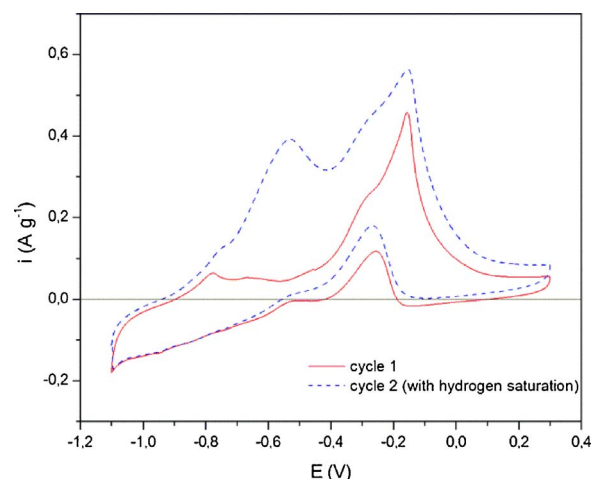


Fig. 10. Cyclic voltammograms recorded for $\text{NiCl}_2\text{-FeCl}_3\text{-PdCl}_2\text{-EGIC}$ in 6 M KOH solution with and without addition of methanol accompanied by the 15 min hydrogen saturation of electrode at -1.1 V . Scan rate 10 mV s^{-1} .

superposition of peaks associated with hydrogen desorption and methanol oxidation it is difficult to precisely determine exact anodic charge of alcohol oxidation. Taking into account that the process of methanol oxidation occurs within the potential range of $-0.42\text{--}0.1 \text{ V}$, the increase in anodic charges for GIC and EGIC are closed to 27% (from 0.55 to 0.70 C g^{-1}) and 67% (from 10.47 to 17.49 C g^{-1}), respectively.

Not-less-interesting result is that the anodic peak associated with Pd catalyst reactivation recorded during the cathodic polarization also increases. This effect is much more pronounced on the curve obtained for chemically exfoliated compound (Fig. 10).

The above described increase in catalytic activity can be ascribed to active hydrogen (H^\bullet) present/sorbed onto the Pd intercalate participating in the reactivation of the palladium catalyst by the removal of poisoning CO species being intermediate products of methanol oxidation [38]. The impact of sorbed hydrogen on the improvement of electrocatalytic activity towards alcohol oxidation was described in our previous work focused on the electrochemical oxidation of methanol onto Ni foam/palladium electrodes [39]. The similar behavior was shown by Yépez and Scharifker in work devoted to oxidation of formate onto Pd catalyst [40].

4. Conclusions

The XRD analysis revealed that the obtained graphite intercalation compound with nickel, iron and palladium chlorides is a mixture of stage-3, 4 compound. This analysis proved that despite the fact that the intercalate molecules remains within the graphitic matrix, chemical exfoliation leads to changes in its structure.

The exfoliation of $\text{NiCl}_2\text{-FeCl}_3\text{-PdCl}_2\text{-GIC}$ results in changes of its morphology due to a partial splitting and wrinkling of graphite flakes, thus leading to the formation of product with accordion-like structure. TEM images revealed that intercalate molecules with diameters varying from 1 nm to 100 nm are evenly distributed on the graphite flakes of exfoliated compound.

SEM analysis together with calculation of BET surface area showed morphological and structural differences between the both investigated materials.

Electrochemical measurements conducted by cyclic voltammetry method revealed 15-fold increase in the catalytic activity of $\text{NiCl}_2\text{-FeCl}_3\text{-PdCl}_2\text{-EGIC}$ towards the methanol electrooxidation. Such a behavior can be explained in term of structure opening effect caused by its chemical exfoliation. The positive influence of exfoliation process on the electrocatalytic activity of $\text{NiCl}_2\text{-FeCl}_3\text{-PdCl}_2\text{-GIC}$ was also confirmed by potentiostatic measurements performed at 0.6 V.

Long-term CV measurements showed successive increment in electrochemical activity for GIC and EGIC toward the methanol oxidation upon cycling. This behavior is most likely associated with the improvement of electrodes wettability among cycling and/or process of their electrochemical exfoliation.

Additionally, CV investigations indicated increased catalytic activity of the original GIC as well as chemically exfoliated GIC towards methanol oxidation in correlation with the process of hydrogen sorption/desorption. This can be explained by the reaction of active hydrogen radicals with intermediates of methanol oxidation i.e. CO causing the reactivation of Pd catalyst surface.

Acknowledgment

This work was supported by Poznan University of Technology research grant no. 03/31/0335/2017-DS-PB.

References

- [1] H. Liu, J. Zhang, *Electrocatalysis of Direct Methanol Fuel Cells*, Wiley-VCH Verlag GmbH & Co., Weinheim, 2009.
- [2] M. Shao, *Electrocatalysis in Fuel Cells: A Non- and Low-Platinum Approach*, Springer-Verlag, London, 2013.
- [3] S.S. Munjewar, S.B. Thombre, R.K. Mallick, A comprehensive review on recent material development of passive direct methanol fuel cell, *Ionics* 23 (2017) 1–18.
- [4] H. Lei, P. Atanassova, Y. Sun, B. Blizanac, State-of-the-art electrocatalysis of direct methanol fuel cells, in: H. Liu, J. Zhang (Eds.), *Electrocatalysis of Direct Methanol Fuel Cells*, Wiley-VCH Verlag GmbH & Co., Weinheim, 2009, pp. 197–226.
- [5] S. Wasmus, A. Küver, Methanol oxidation and direct methanol fuel cells: a selective review, *J. Electroanal. Chem.* 461 (1999) 14–31.
- [6] H. Liu, Ch. Song, L. Zhang, J. Zhang, H. Wang, D.P. Wilkinson, A review of anode catalysis in the direct methanol fuel cell, *J. Power Sources* 155 (2006) 95–110.
- [7] R.N. Singh, A. Singh, Anindita, Electrocatalytic activities of binary and ternary composite electrodes of Pd, nanocarbon and Ni for electro-oxidation of methanol in alkaline medium, *J. Solid State Electrochem.* 13 (2009) 1259–1265.
- [8] H.S. Thiam, W.R.W. Daud, S.K. Kamarudin, A.B. Mohamad, A.A.H. Kadhum, K.S. Loh, E.H. Majlan, Performance of direct methanol fuel cell with a palladium–silica nanofibre/naion composite membrane, *Energy Convers. Manag.* 75 (2013) 718–726.
- [9] J.C.C. Gómez, R. Moliner, M.J. Lázaro, Palladium-based catalysts as electrodes for direct methanol fuel cells: a last ten years review, *Catalysts* 6 (9) (2016) 130.
- [10] T. Jurzinsky, P. Kammerer, C. Cremers, K. Pinkwart, J. Tübke, Investigation of ruthenium promoted palladium catalysts for methanol electrooxidation in alkaline media, *J. Power Sources* 303 (2016) 182–193.
- [11] E. Antolini, E.R. Gonzalez, Alkaline direct alcohol fuel cells, *J. Power Sources* 195 (2010) 3431–3450.
- [12] R. Kazemi, A. Kiani, Deposition of palladium submonolayer on nanoporous gold film and investigation of its performance for the methanol electrooxidation reaction, *Int. J. Hydrogen Energy* 37 (2012) 4098–4106.
- [13] M. Zhiani, B. Rezaei, J. Jalili, Methanol electro-oxidation on Pt/C modified by polyaniline nanofibers for DMFC applications, *Int. J. Hydrogen Energy* 35 (2010) 9298–9305.
- [14] J. Sun, M. Dou, Z. Zhang, J. Ji, F. Wang, Carbon nanotubes supported Pt-Co-P ultrafine nanoparticle electrocatalysts with superior activity and stability for methanol electro-oxidation, *Electrochim. Acta* 215 (2016) 447–454.
- [15] P. Krawczyk, T. Rozmanowski, M. Osińska, Electrochemical sorption of hydrogen in exfoliated graphite/nickel/palladium composite, *Int. J. Hydrogen Energy* 41 (2016) 20433–20438.
- [16] M.S. Dresselhaus, G. Dresselhaus, Intercalation compounds of graphite, *Adv. Phys.* 51 (2002) 1–187.
- [17] M. Inagaki, *Intercalation Compounds*, Elsevier Science Ltd., Oxford, 2000.
- [18] H. Shioyama, Reactions of chlorine and related molecules with graphite intercalation compounds, *J. Phys. Chem. Solids* 67 (2006) 1447–1450.
- [19] A.V. Dunaev, I.V. Arkhangelsky, Y.V. Zubavichus, V.V. Avdeev, Preparation, structure and reduction of graphite intercalation compounds with hexachloroplatinic acid, *Carbon* 46 (2008) 788–795.
- [20] M. Inagaki, Z.D. Wang, Y. Okamoto, M. Ohira, The synthesis of $\text{NiCl}_2\text{-FeCl}_3\text{-graphite}$ intercalation compounds, *Synth. Met.* 20 (1987) 9–13.
- [21] O.N. Shornikova, A.V. Dunaev, N.V. Maksimova, V.V. Avdeev, Synthesis and properties of ternary GIC with iron or copper chlorides, *J. Phys. Chem. Solids* 67 (2006) 1193–1197.
- [22] T. Rozmanowski, P. Krawczyk, Changes in structure, morphology and electrochemical properties of $\text{NiCl}_2\text{-FeCl}_3\text{-PdCl}_2\text{-graphite}$ intercalation compound affected by gaseous hydrogen reduction process, *Electrochim. Acta* 205 (2016) 266–272.
- [23] J.M. Skowroński, Graphite intercalation compounds, in: H.S. Nalwa (Ed.), *Handbook of Organic Conductive Molecules and Polymers*, John Wiley and Sons Ltd., Chichester, 1997, pp. 621–686.
- [24] H.M.A. Asghar, S.N. Hussain, H. Sattar, N.W. Brown, E.P.L. Roberts, Potential graphite materials for the synthesis of GICs, *Chem. Eng. Commun.* 202 (2015) 508–512.
- [25] J.M. Skowroński, T. Rozmanowski, P. Krawczyk, Enhancement of electrochemical hydrogen storage in $\text{NiCl}_2\text{-FeCl}_3\text{-PdCl}_2\text{-graphite}$ intercalation compound effected by chemical exfoliation, *Appl. Surf. Sci.* 275 (2013) 282–288.
- [26] E. Bourelle, B. Claude-Montigny, A. Metrot, Electrochemical exfoliation of HOPG in formic-sulfuric acid mixtures, *Mol. Cryst. Liq. Cryst.* 310 (1998) 321–326.
- [27] J.M. Skowroński, P. Krawczyk, T. Rozmanowski, J. Urbaniak, Electrochemical behavior of exfoliated $\text{NiCl}_2\text{-graphite}$ intercalation compound affected by hydrogen sorption, *Energy Convers. Manag.* 49 (2008) 2440–2446.
- [28] D.D.L. Chung, Exfoliation of graphite, *J. Mater. Sci.* 22 (1987) 4190–4198.
- [29] G. Furdin, Exfoliation process and elaboration of new carbonaceous materials, *Fuel* 77 (1998) 479–485.
- [30] J.M. Skowroński, P. Krawczyk, Modification of expanded graphite resulting in enhancement of electrochemical activity in the process of phenol oxidation, *J. Appl. Electrochem.* 40 (2010) 91–98.
- [31] A. Czerwiński, I. Kiersztyn, M. Grdeń, The study of hydrogen sorption in palladium limited volume electrodes (Pd-LVE) Part II. Basic solutions, *J. Electroanal. Chem.* 492 (2000) 128–136.
- [32] K. Hubkowska, M. Łukaszewski, A. Czerwiński, Influence of temperature on hydrogen electrosorption into palladium–noble metal alloys. Part 1: palladium–gold alloys, *Electrochim. Acta* 56 (2010) 235–242.
- [33] S.R. Chowdhury, P. Mukherjee, S.K. Bhattacharya, Palladium and palladium-copper alloy nanoparticles as superior catalyst for electrochemical oxidation of methanol for fuel cell applications, *Int. J. Hydrogen Energy* 41 (2016) 17072–17083.
- [34] J. Fan, K. Qi, H. Chen, W. Zheng, X. Cui, Morphology dependence of electrochemical properties on palladium nanocrystals, *J. Colloid Interface Sci.* 490 (2017) 190–196.
- [35] K.S. Kumar, P. Haridoss, S.K. Seshadri, Synthesis and characterization of electro-deposited Ni–Pd alloy electrodes for methanol oxidation, *Surf. Coat. Technol.* 202 (2008) 1764–1770.
- [36] K. Hubkowska, U. Koss, M. Łukaszewski, A. Czerwiński, Hydrogen electrosorption into Pd-rich Pd–Ru alloys, *J. Electroanal. Chem.* 704 (2013) 10–18.
- [37] A. Zalineaeva, S. Baranton, Ch. Coutanceau, G. Jerkiewicz, Octahedral palladium nanoparticles as excellent hosts for electrochemically adsorbed and absorbed hydrogen, *Sci. Adv.* 3 (2017) e1600542.
- [38] O. Yépez, G. Pickup, Electrochemical oxidation of methanol at hydrogen-loaded PdPtRu-coated Pd electrodes, *Electrochim. Solid State Lett.* 8 (2005) E35–E38.
- [39] O. Yépez, B.R. Scharifker, Oxidation of formate on hydrogen-loaded palladium, *Int. J. Hydrogen Energy* 27 (2002) 99–105.
- [40] J.M. Skowroński, T. Rozmanowski, Relationship between the reactions of hydrogen sorption/desorption and methanol oxidation on bifunctional Ni/Pd electrode in alkaline solution, *J. Solid State Electrochem.* 17 (2013) 949–960.